Textured Superconducting Phase in the Heavy Fermion CeRhIn_{5}

Tuson Park, H. Lee, I. Martin, X. Lu, V. A. Sidorov, K. Gofryk, F. Ronning, E. D. Bauer, and J. D. Thompson

Phys. Rev. Lett. **108**, 077003 — Published 14 February 2012

DOI: 10.1103/PhysRevLett.108.077003

Textured Superconducting State in the Heavy Fermion $CeRhIn_5$

Tuson Park,[1,2] H. Lee,[2,*] I. Martin,[2] X. Lu,[2] V. A. Sidorov,[2,3]
K. Gofryk,[2] F. Ronning,[2] E. D. Bauer,[2] and J. D. Thompson[2]

[1] *Department of Physics, Sungkyunkwan University, Suwon 440-746, Korea*
[2] *Los Alamos National Laboratory, Los Alamos, New Mexico 87545, USA*
[3] *Vereshchagin Institute of High Pressure Physics, RAS, 142190 Troitsk, Russia*

When antiferromagnetism and unconventional superconductivity coexist in $CeRhIn_5$, there is a significant temperature difference between resistively- and thermodynamically-determined transitions into the superconducting state. In this state, anisotropic transport near the superconducting transition reveals the emergence of textured superconducting planes that appear without a change in translational symmetry of the lattice. $CeRhIn_5$ is not unique in exhibiting these behaviors, indicating that textured superconductivity may be a general consequence of coexisting orders in correlated electron materials.

PACS numbers: 74.70.Tx, 71.27.+a, 74.25.Fy, 74.62.Fj

Anisotropic, spatially textured electronic states often emerge when the symmetry of the underlying crystalline structure is lowered [1]. The possibility, however, has been raised that novel electronic quantum states with real-space texture could arise in strongly correlated systems even without changing the underlying crystalline structure [2–5]. The appearance of unexpected anisotropy in electrical resistivity has been particularly useful for signalling the presence of these novel states, but in many cases, their relation to coexisting broken symmetries, such as magnetism or superconductivity, remains unknown, in part because these states often are accessed by introducing chemical and associated structural disorder.

The cuprate superconductors are a notable example in which real-space electronic texture emerges out of strong correlations [2]. Except for possibly the 'hidden order' state in URu_2Si_2 [6], the possibility of a textured electronic phase in heavy-fermion systems has not been considered, even though they are prototypes of strong electronic correlations. $CeRhIn_5$ is one of those materials. At ambient pressure, its Ce-derived 4f-moments order antiferromagnetically at $T_N = 3.7$ K, above which the large Sommerfeld coefficient of specific heat γ ($\approx$ 400 mJ/molK^2) is characteristic of heavy quasiparticles [7, 8]. Application of pressure to $CeRhIn_5$ induces a phase of microscopically coexisting antiferromagnetic order and bulk, unconventional (d-wave) superconductivity for a range of pressures below P_{c1}(=1.75 GPa), above which magnetism disappears but superconductivity remains [9–11]. The width ΔT_c of the resistive transition to superconductivity varies strongly with pressure: below P_{c1} , the in-plane resistivity ρ_{ab} goes to zero at 1.25 K with $\Delta T_c = 0.95$ K at 1.6 GPa, but $\Delta T_c \leq 0.01$ K above P_{c1} (refs. [12, 13]). The residual resistivity ratio, $\rho_{ab}(300K)/\rho_{ab}(0K) \approx 1000$, is exceptionally large, implying very homogenous crystallinity and that the large ΔT_c below P_{c1} is not due to poor sample quality but rather suggests the possibility of a new electronic state. To explore the origin of the broad SC transition, we measured specific heat of $CeRhIn_5$ and its electrical resistivity under pressure for electrical current applied along different crystalline axes. In the coexisting phase, ρ_c sharply goes to zero while ρ_{ab} shows a broad tail. As will be discussed, additional anisotropic transport within the Ce-In plane is consistent with the emergence of textured superconducting planes that are formed preferentially along {100} planes. Disappearance of the anisotropic transport near T_c for $P > P_{c1}$ suggests that the textured SC planes are a consequence of the competing orders of antiferromagnetism and superconductivity.

Single crystals of $CeRhIn_5$ were synthesized by the In-rich flux method [7]. Crystals were screened by resistivity and susceptibility measurements that showed no detectable free In within the resolution of susceptibility ($\approx$ 0.02% volume percent). A conventional four-point contact technique was used to measure the electrical resistivity of $CeRhIn_5$, where samples were polished into bar shapes for different geometry with current being applied along the elongated direction. Specific heat measurements under pressure were performed via ac calorimetry technique [14]. Quasi-hydrostatic pressure environments were produced by using silicone fluid and glycerol-water mixture (60/40) as the pressure transmitting medium for pressures up to 3 GPa in a clamp-type cell and up to 5.23 GPa in a toroidal cell, respectively. Pressures at low temperatures were determined resistively via the suppression of the superconducting transition temperature of Sn or Pb (ref. [15]).

Figure 1 plots the low-temperature specific heat divided by temperature and in-plane resistivity ρ_{ab} of $CeRhIn_5$ at pressures of 1.58, 1.70, 2.20 GPa in panels a, b, and c, respectively. At 1.58 GPa, the specific heat shows well-defined anomalies near 2.6 and 1.3 K that correspond to Néel order and to the subsequent bulk superconducting transition T_c. The in-plane resistivity, in contrast, reveals three characteristic temperatures of $T_N = 2.6$, $T_\rho = 2.0$, and $T_c = 1.26$ K that are asso-

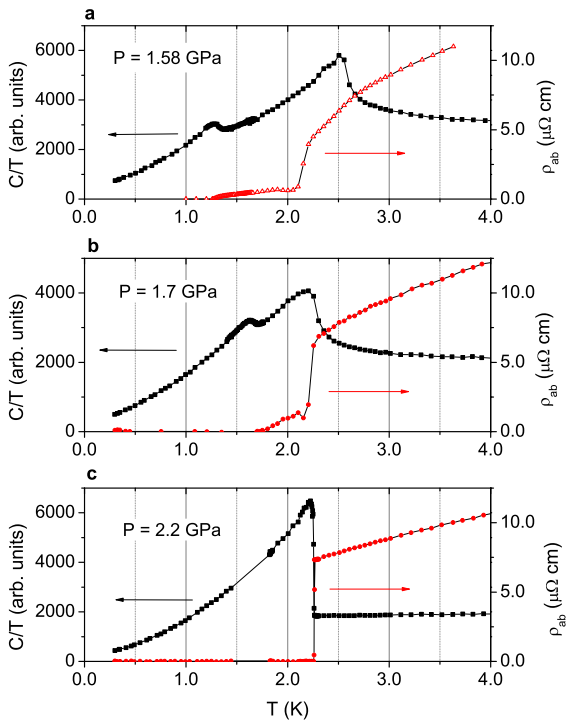

FIG. 1: (color online) Specific heat divided by temperature (C/T) and in-plane electrical resistivity (ρ_{ab}) of $CeRhIn_5$ as a function of temperature. C/T and ρ_{ab} are plotted on the left and right ordinates, respectively. Panels display the data for pressures of 1.58, 1.7, and 2.2 GPa in **a**, **b**, and **c**. At 1.58 and 1.7 GPa, anomalies in C/T at high temperature denote the formation of long-range magnetic order and those at lower temperature are due to bulk superconductivity. The single anomaly in C/T at 2.2 GPa ($> P_{c1}$) signals the development of superconductivity.

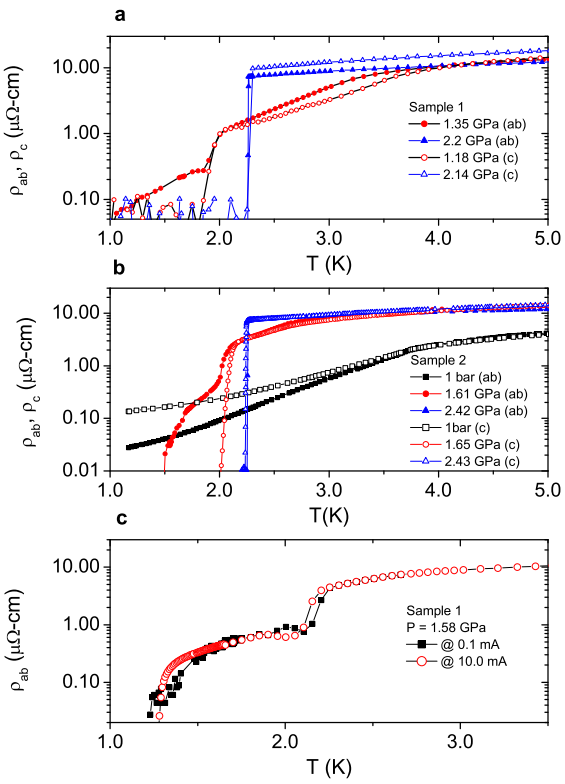

FIG. 2: (color online) Electrical resistivity of $CeRhIn_5$ for current parallel (open symbols) and perpendicular (solid symbols) to the crystalline c-axis. Data from single crystals of $CeRhIn_5$ from batch numbers 1 and 2 are shown in **a** and **b**, respectively. Anisotropy at 1 bar in panel **b** is associated with antiferromagnetic order. **c** The in-plane electrical resistivity ρ_{ab} on a semi-logarithmical scale as a function of temperature for applied currents of 0.1 (solid squares) and 10 mA (open circles) at 1.58 GPa.

ciated with Néel ordering, a dip in the resistivity, and zero resistance, respectively. T_ρ, clearly a signature of superconductivity, differs significantly from the thermodynamic T_c [16, 17]. Instead of going to zero directly, ρ_{ab} shows a long tail of finite resistance down to 1.26 K, the thermodynamic SC transition temperature. The difference $T_\rho - T_c$ inferred from the data shown in Fig. 1 decreases with pressure and becomes negligible above P_{c1}, indicating that the finite width is related to the presence of the antiferromagnetic order. Scaling of the characteristic temperatures with magnetic field evidences that the same electrons are responsible for the onset, dip, and zero resistance states (not shown).

Anisotropy between in-plane (ρ_{ab}) and out-of-plane resistivity (ρ_c) is plotted as a function of temperature for different pressures in Fig. 2a. Extrapolating these curves to $T = 0$ at ambient pressure gives residual values for ρ_{ab} and ρ_c of 7.9 ± 0.5 and 90 ± 7 nΩ·cm, respectively. If the shoulder-like broad SC transition region were due to sample inhomogeneity or disorder, it would be more prominent for ρ_c because its residual value is much larger than that of ρ_{ab}. Contradicting this expectation, however, ρ_c sharply goes to zero, but ρ_{ab} has an extended tail down to the bulk T_c. For $P > P_{c1}$, both ρ_c and ρ_{ab} go to zero simultaneously. Even though the detailed temperature dependence of the shoulder-like feature in the SC region of ρ_{ab} is sample dependent, the overall characteristic features in the resistivity of $CeRhIn_5$ are reproducible as seen in a comparison of Figs. 2a and 2b. When the electrical current used to measure ρ_{ab} is varied from 0.1 to 10 mA (see Fig. 2c), a factor of 10^6 change in the input power, the onset of filamentary superconductivity varies slightly due to pair-breaking, but the shoulder-like behavior persists, confirming the intrinsic nature of the anisotropic resistance-T_c anomaly.

The disappearance of anisotropy in the resistive transition as well as the coincidence of thermodynamic and resistive transitions above P_{c1} suggest that filamentary superconductivity does not arise from internal structural strains or defects because hydrostatic pressure has no or little effect on these hypothetical extrinsic contributions.

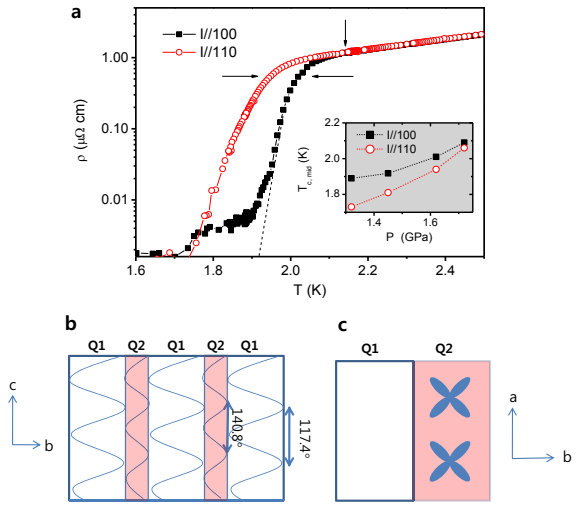

FIG. 3: (color online) **a** The in-plane electrical resistivity of $CeRhIn_5$ at 1.45 GPa for current applied along [100] (solid squares) and [110] (open circles). For these experiments, two samples were prepared by cutting one crystal into two pieces, each with different crystallographic orientations. The minimum measurable resistivity of 1.8 nΩ·cm is taken to be zero resistance. Inset: Pressure evolution of $T_{c,mid}$ for the two current directions [100] and [110]. $T_{c,mid}$, defined as the temperature at which the resistivity drops to 50 % of its normal state value, is marked by side arrows and the onset of the SC transition is indicated by a vertical arrow. Dashed lines are guides to eyes. **b** Schematic illustration of the spatial variation of the amplitude of the textured superconducting state with respect to antiferromagnetic phases with antiferromagnetic ordering wave vectors of Q1=(1/2, 1/2, 0.326) and Q2=(1/2, 1/2, 0.391), respectively. The lines inside the domain describe spatial rotation of the Ce 4f spins, which shows the different pitch angles within the incommensurate Q1 and Q2 phases. **c** Illustration of the superconducting d-wave order parameter inside Q2+SC domains.

Recent neutron scattering measurements have shown, however, that below P_{c1} a new incommensurate magnetic structure Q2 = (1/2, 1/2, 0.391) starts to appear below a characteristic temperature T^* and completely replaces the original one with Q1 = (1/2, 1/2, 0.326) below the bulk superconducting transition temperature T_c (ref. [18]). The coincidence of T^* with the resistive superconducting onset temperature suggests formation of lamellar superconductivity residing either in the magnetic domain walls or in the nucleated domains of Q2. From the rapid decrease of ρ_c but broad transition in ρ_{ab}, we conclude that the domains are preferentially oriented along the c-axis. Though superconductivity might nucleate first at the domain walls, where both Q1 and Q2 magnetic phases coexist, the observation that the bulk T_c coincides with the transition to the uniform Q2 phase implies that Q2 domains can also support SC.

Figure 3 shows the temperature-dependent resistivity of $CeRhIn_5$ at a representative pressure for electrical current applied along [100] and [110] directions. Even though the onset and zero-resistivity temperatures of the SC transition occur simultaneously for both current directions, the temperature dependence of the transition differs significantly: [100] initially drops sharply, shows a plateau, and then decreases to the instrumental resolution at 1.7 K, which we take as zero resistance. In contrast, [110] gradually goes to zero at 1.7 K. The in-plane superconducting anisotropy characterized by the temperature $T_{c,mid}$ and plotted in the inset to Fig. 3b, becomes smaller upon approaching P_{c1} and disappears above P_{c1}. The in-plane resistive anisotropy implies breaking of rotational symmetry, with the transition for current flow along [110] being distinct from that of [100] below the resistive SC transition temperature. This is unexpected considering that $CeRhIn_5$ is tetragonal throughout the whole temperature range. A state consistent with these observations is a lamellar structure of Q2 + SC planes embedded in a Q1 matrix. There can be two reasons for anisotropy: either it is caused by non-linear effects in resistivity, or it is due to the presence of domains of size comparable to the sample dimension. Indeed, if the characteristic Q2+SC domain size were much smaller than crystal dimensions, the tetragonal symmetry of $CeRhIn_5$ would not be broken on a macroscopic scale. In this case, the linear resistivity within the ab-plane must be isotropic; in particular, $\rho_{[110]} = \rho_{[100]}$ and any anisotropy could come only from higher order in current terms in resistivity. However, as is shown in Fig. 4, even in the limit of zero applied current, the resistivities in [100] and [110] directions are different, which indicates that the anisotropy is not a result of a non-linear response. Therefore, it must reflect the domain structure with a characteristic length scale comparable to the sample size. If we assume that the magnetic transition from Q1 to Q2 favors formation of domain walls (and hence also domains of Q2+SC) along [100] and [010], then the superconducting sheets will run diagonally to the long axis of the sample oriented along [110] and predominantly parallel to the long axis for sample oriented along [100] (since domain nucleation is biased by the sample surface). In the former case there will be no direct path connecting the current source and drain, but in the latter there will. This naturally leads to $\rho_{[100]} < \rho_{[110]}$, as is observed experimentally.

Striking anisotropy in the superconducting transition of $CeRhIn_5$ suggests the existence of an intrinsic, intermediate region between the bulk and transport T_c's, where the SC state is textured in real space due to a coexisting electronic phase, which in the case of $CeRhIn_5$ is magnetism. Though the study of $CeRhIn_5$ has revealed this texture, it is reasonable to suspect that this example is not unique. Indeed, it should be a general feature of strongly correlated electron superconductors in which there is a coexisting order. Indeed, similar SC transition patterns are observed when the competing phase is magnetism with incommensurate local mo-

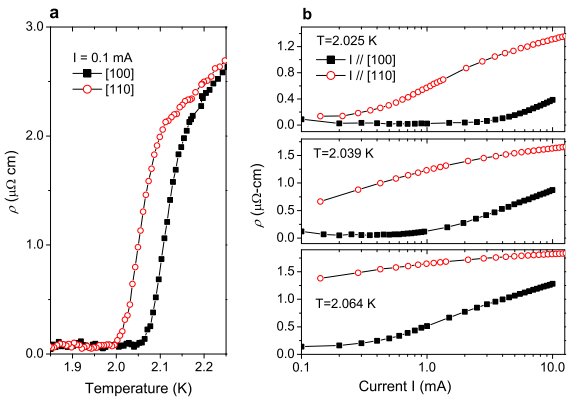

FIG. 4: (color online) **a** Electrical resistivity of $CeRhIn_5$ at 1.76 GPa as a function of temperature in the superconducting transition region. Solid and open symbols represent the resistivity for current flow of 0.1 mA along [100] and [110], respectively. **b** Resistivity of $CeRhIn_5$ at 1.76 GPa as a function of applied current for current flow along [100] (solid symbols) and [110] (open symbols) in the superconducting transition region at temperatures indicated in each panel.

ment order ($CeRhIn_5$), strong commensurate order (Cd-doped $CeCoIn_5$), weak incommensurate density wave order (A/S $CeCu_2Si_2$), in a superconductor without inversion symmetry ($CePt_3Si$) or in a different class of superconductors (Co-doped $BaFe_2As_2$) with density-wave order [19–23]. Experimental evidence from these references is given in the Supplemental Material [24]. Interestingly, as shown by $CeIrIn_5$ and $La_{1-x}Ba_xCuO_4$ ($x = 1/8$), long-range competing magnetic order is not a strict prerequisite for separating bulk and transport transition temperatures [25–27]. The observation that an anomalous resistive transition is most prominent in high-quality samples but vanishes in lower-quality specimens contradicts the conventional interpretation that these effects are due to disorder and requires a more fundamental explanation. Experiments, such as those discussed, will reveal details of the coupling and interplay of these orders.

Work at Los Alamos was performed under the auspices of the U.S. Department of Energy, Office of Science, Division of Materials Science and Engineering and supported in part by the Los Alamos LDRD program. TP acknowledges a support by Basic Science Research Program (No 2010-002672) and Mid-career Researcher Program (No 2010-0029136) through the National Research Foundation (NRF) funded by Korea government (MEST). VAS acknowledges a support from the Russian Foundation for Basic research (grant 09-02-00336).

* Present address: Department of Applied Physics and Geballe Laboratory for Advanced Materials, Stanford University, Stanford, California 94305, USA

[1] E. Fradkin, S. A. Kivelson, M. J. Lawler, J. P. Eisenstein, and A. P. Mackenzie, Annu. Rev. Condens. Matter Phys. **1**, 153 (2010).
[2] S. A. Kivelson, E. Fradkin, and V. J. Emery, Nature **393**, 550 (1998).
[3] R. A. Borzi *et al.*, Science **315**, 214 (2007).
[4] Y. Ando, K. Segawa, S. Komiya, and A. N. Lavrov, Phys. Rev. Lett. **88**, 137005 (2002).
[5] T.-M. Chuang *et al.*, Science **327**, 181 (2010).
[6] C. M. Varma and Lijun Zhu, Phys. Rev. Lett. **96**, 036405 (2006).
[7] H. Hegger *et al.*, Phys. Rev. Lett. **84**, 4986 (2000).
[8] W. Bao *et al.*, Phys. Rev. B **65**, 100505(R) (2002).
[9] T. Mito *et al.*, Phys. Rev. B **63**, 220507 (2001).
[10] Y. Korori,Y. Yamato, Y. Iwamoto, and T. Kohara, Eur. Phys. J. B **18**, 601 (2000).
[11] S. Kawasaki *et al.*, Phys. Rev. B **65**, 020504 (2001).
[12] T. Park *et al.*, J. Phys.: Condens. Matter **23**, 094218 (2011).
[13] T. Park, M. J. Graf, L. Boulaevski, J. L. Sarrao, and J. D. Thompson, Proc. Nat. Acad. Sci. **105**, 6825 (2008).
[14] Y. Kraftmakher, Phys. Rep. **356**, 1 (2001).
[15] A. Eiling and J. S. Schilling, J. Phys. F: Metal Phys. **11**, 623 (1981).
[16] G. Knebel, D. Aoki, D. Braithwaite, B. Salce, and J. Flouquet, Phys. Rev. B **74**, 020501(R) (2006).
[17] T. Park, F. Ronning, H. Q. Yuan, M. B. Salamon, R. Movshovich, J. L. Sarrao, and J. D. Thompson, Nature **440**, 65 (2006).
[18] N. Aso *et al.*, J. Phys. Soc. Jpn. **78**, 073703 (2009).
[19] L. D. Pham, T. Park, S. Maquilon, J. D. Thompson, and Z. Fisk, Phys. Rev. Lett. **97**, 056404 (2006).
[20] F. Steglich *et al.*, Phys. Rev. Lett. **43**, 1892 (1979).
[21] E. Lengyel, Thesis (Max-Planck-Institute, Dresden, Germany) (2007).
[22] T. Takeuchi *et al.*, J. Phys. Soc. Jpn. **76**, 014702 (2007).
[23] K. Gofryk *et al.*, (unpublished).
[24] See Supplemental Material for data and their discussion.
[25] Q. Li, M. Hucker, G. D. Gu, A. M. Tsvelik, and J. M. Tranquada, Phys. Rev. Lett. **99**, 067001 (2007).
[26] J. M. Tranquada *et al.*, Phys. Rev. B **78**, 174529 (2008).
[27] C. Petrovic *et al.*, Europhys. Letts. **53**, 354 (2001).